SF2A 2015
F. Martins, S. Boissier, V. Buat, L. Cambrésy and P. Petit (eds)

AGN FEEDBACK AND JET-INDUCED STAR FORMATION

Q. Salomé[1], P. Salomé[1], F. Combes[1 2] and S. Hamer[1]

Abstract. We studied the impact of the AGN in radio galaxies on star formation along the radio jet. Our main goal was to determine whether star formation is more efficient in the shocked region along the jet.

A first large scale work based on IRAM-30m CO observations of 3C 285 and Minkowski's Object has shown the star-forming spots located a few tens of kpc along the radio jet appears to form stars at least as efficiently as typical spiral galaxies or even boosted. This result supports the AGN positive feedback scenario.

On the opposite, a small scale multi-wavelength analysis of the northern filaments of Centaurus A tends to quench star formation in the filaments, maybe due to the AGN negative feedback.

Keywords: Methods:data analysis, Galaxies:evolution, interactions, star formation, Radio lines:galaxies

1 Introduction

AGN are thought to play a role in galaxy evolution (and formation), but it is yet not clear how the so-called AGN feedback affects star formation. On the one hand, a *negative* feedback could prevent or regulate star formation through the energy released by the AGN (Heckman & Best 2014 and references therein). On the other hand, it is expected that the propagation of jet-driven shocks can accelerate the gas cooling and trigger star formation (Best & Heckman 2012; Ivison et al. 2012), producing an AGN *positive* feedback.

Leroy et al. (2008, 2013) compared the molecular gas content of nearby galaxies with SFR tracers. They found that the star formation efficiency depends mostly if not only on the amount of molecular gas. However, some environmental effects may also influence star formation (Daddi et al. 2010; Genzel et al. 2010).

Evidence of jet-induced star formation has been claimed only for a few objects: (1) Centaurus A (Schiminovich et al. 1994; Charmandaris et al. 2000); (2) Minkowski Object (van Breugel et al. 1985); (3) 3C 285 (van Breugel & Dey 1993); (4) at z = 3.8, the radio source 4C 41.17 (Bicknell et al. 2000; De Breuck et al. 2005; Papadopoulos et al. 2005).

To better understand the impact of the AGN interaction with the intergalactic medium on star formation, we conducted two studies at large (3C 285 and Minkowski's Object) and small scales (the northern filaments of Centaurus A). Our main goal was to determine whether star formation is more efficient in the shocked region along the jet. Throughout this work, we assume the cold dark matter concordance Universe, with $H_0 = 70 \mathrm{km.s^{-1}.Mpc^{-1}}$, $\Omega_\mathrm{m} = 0.30$ and $\Omega_\mathrm{A} = 0.70$.

2 Hint of jet-induced star formation in 3C 285 and Minkowski's object

3C 285 is a double-lobed powerful FR-II radio galaxy where both lobes have a complex filamentary structure. In the eastern radio lobe, there is a radio jet with unresolved radio knots. A slightly resolved object in Hα emission is located near the eastern radio jet (**3C 285/09.6**; van Breugel & Dey 1993). 3C 285/09.6 is a small, kiloparsec-sized object where star formation seems to be triggered by the jet.

Minkowski's Object (MO) is a star-forming peculiar object near the double-lobed FR-I radio source NGC 541 in the galaxy cluster Abell 194 (Croft et al. 2006), located in a large optical bridge that connects NGC 541 with the interacting galaxies NGC 545/547. VLA observations show two HI clouds "wrapped" around the eastern jet with a total HI mass of 4.9×10^8 $M_\odot$ (Croft et al. 2006).

We have observed the CO(1-0) and CO(2-1) emission along the jet axis of the radio galaxies 3C 285 and NGC 541. The observations were made with the IRAM 30m telescope on March and June 2014, using the EMIR receiver with the

[1] LERMA, Observatoire de Paris, CNRS UMR 8112, 61 avenue de l'Observatoire, 75014 Paris, France
[2] Collège de France, 11 place Marcelin Berthelot, 75005 Paris

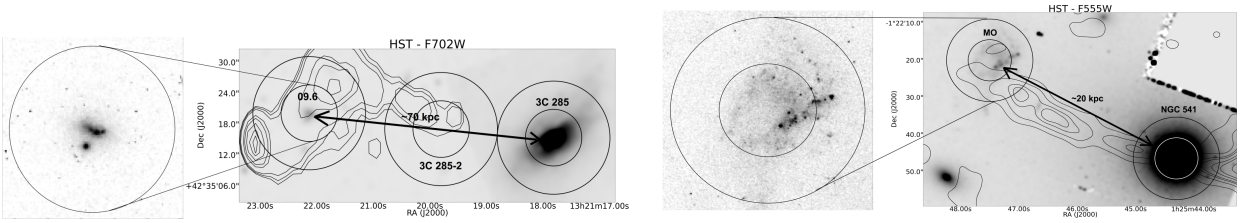

Fig. 1: Contour map of 3C 285 and NGC 541 observed at 21 cm (van Breugel & Dey 1993; van Breugel et al. 1985), overlaid on a slightly smoothed optical image. The observed positions are shown by the CO(1-0) and CO(2-1) IRAM 30m beams (circles). Details of 3C 285/09.6 and Minkowski's Object.

WILMA backend (bandwidth of 3.7 GHz; resolution of 2 MHz). Three regions were observed in March 2014: the central galaxy 3C 285, 3C 285/09.6, and an intermediate position (3C 285-2) along the jet (cf. Fig. 1). In June 2014, observations pointed at NGC 541 and Minkowski's Object (cf. Fig. 1).

CO luminosities The central galaxies were detected in both CO(1-0) and CO(2-1), whereas there is no detection for the other positions. Each line was fitted by a gaussian in order to get its characteristics (see Salomé et al. 2015 for the details). The CO luminosity L'_{CO} was calculated with the formula from Solomon et al. (1997) and the molecular gas mass was estimated using a standard Milky Way conversion factor of 4.6 $M_\odot.(K.km.s^{-1}.pc^2)^{-1}$ (Solomon et al. 1997).
Star formation rate and depletion time The Hα and IR emission is often used as tracers of star formation. We derived a star formation rate from the Hα (Baum & Heckman 1989; van Breugel & Dey 1993) and IR emission (computed with Herschel-SPIRE data from the archive), following the methods of Kennicutt & Evans (2012) and Calzetti et al. (2007). The total SFR is the sum of the SFR derived from the Hα and the IR emission. The molecular gas depletion time is the time to consume all the molecular gas with the present star formation rate: $t^{mol}_{depl} \sim M_{H_2}/SFR$.

Source	3C 285	3C 285/09.6	NGC 541	MO
SFR ($M_\odot.yr^{-1}$)	14.53	0.62	0.095	0.47
t_{dep} (Gyr)	0.71	< 1.0	1.79	0.02

Table 1: SFR and depletion for the different objects observed with the IRAM 30m.

A Kennicutt-Schmidt law? We have calculated the gas and SFR surface densities (Σ_{gas}, Σ_{SFR}; the values can be found in Salomé et al. 2015). The Σ_{SFR} vs Σ_{gas} diagram (see figure 2, Bigiel et al. 2008; Daddi et al. 2010), shows that the two star-forming regions 3C 285/09.6 and MO stand at least on or even above the KS-law, with molecular gas depletion time < 1 Gyr in 3C285/09.6 and down to < 20 Myr for the Minkowski's Object in regions of ∼ 36 kpc and ∼ 9 kpc. This supports the AGN positive feedback scenario that predicts an enhanced star formation activity along the shocked region inside the radio-jets.

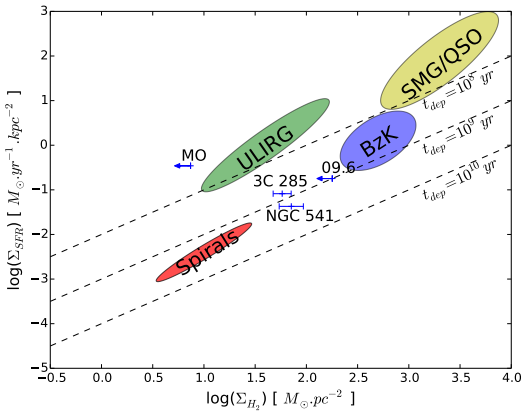

Fig. 2: Σ_{SFR} vs. Σ_{gas} diagram for the sources studied in Salomé et al. (2015). The diagonal dashed lines show lines of constant SF efficiency, indicating the level of Σ_{SFR} needed to consume 1%, 10%, and 100% of the gas reservoir in 10^8 years. Thus, the lines also correspond to constant gas depletion times of, from top to bottom, 10^8, 10^9, and 10^{10} yr The coloured regions come from Daddi et al. (2010).

3 Centaurus A

NGC 5128 (also known as **Centaurus A**) is a giant nearby early type galaxy surrounded by faint arc-like stellar shells (at several kpc around the galaxy). In the shells, HI emission has been detected (Schiminovich et al. 1994) and CO emission was observed at the intersection with the radio jet (Charmandaris et al. 2000). In addition, large amount of dust

($\sim 10^5$ $M_\odot$) lies around the northern shell region (Auld et al. 2012).
Along the radio-jet, optically bright filaments (so-called inner and outer filaments) have been observed (Morganti et al. 1991). These filaments located along the direction of the northern radio jet (at a distance of $\sim$ 7.7 kpc and $\sim$ 13.5 kpc, respectively) are the place of star formation (Auld et al. 2012).

We gathered archival data of the outer filaments in FUV (GALEX), FIR (Herschel) and CO (SEST and ALMA). We also searched for HCN/HCO^+ (ATCA) and observed optical emission lines (VLT/MUSE) in the filaments. Here we summarise the main results of this study, more details can be found in an other SF2A proceeding.

Molecular gas masses of a few $10^5 - 10^6$ $M_\odot$ were detected in several of the 44″ ($\sim$ 0.72 kpc) SEST beam of the map. The Σ_{SFR} vs Σ_{gas} diagram (Bigiel et al. 2008; Daddi et al. 2010) shows that the central galaxy is forming stars very efficiently, similar to ULIRG, whereas star formation at all the CO-SEST positions seems to be **quenched**.

4 Conclusion

CO emission has not been detected by the IRAM 30m telescope in 3C 285/09.6 and Minkoski's Object. Upper limits at 3σ provides molecular gas masses smaller than $\sim 10^7 - 10^8\,M_\odot$. These masses lead to molecular depletion times ≤ 1 Gyr and ≤ 0.02 Gyr, respectively. In addition, the KS-diagram indicates that the star formation is at least as efficient as inside spiral galaxies and even boosted in the case of MO.

Using a standard conversion factor, the whole region of Centaurus A northern filaments contains $M_{H_2} = 2 \times 10^7$ $M_\odot$ with a very long depletion time $t_{dep} \sim 10$ Gyr.

Both objects have different behaviours, leading to a hint of environmental effects. This study is the first step towards a detailed understanding of the feedback effect.

References

Auld, R., Smith, M. W. L., Bendo, G., et al. 2012, MNRAS, 420, 1882
Baum, S. A. & Heckman, T. 1989, ApJ, 336, 681
Best, P. N. & Heckman, T. M. 2012, MNRAS, 421, 1569
Bicknell, G. V., Sutherland, R. S., van Breugel, W. J. M., et al. 2000, ApJ, 540, 678
Bigiel, F., Leroy, A., Walter, F., et al. 2008, AJ, 136, 2846
Calzetti, D., Kennicutt, R. C., Engelbracht, C. W., et al. 2007, ApJ, 666, 870
Charmandaris, V., Combes, F., & van der Hulst, J. M. 2000, A&A, 356, L1
Croft, S., van Breugel, W., de Vries, W., et al. 2006, ApJ, 647, 1040
Daddi, E., Elbaz, D., Walter, F., et al. 2010, ApJ, 714, L118
De Breuck, C., Downes, D., Neri, R., et al. 2005, A&A, 430, L1
Genzel, R., Tacconi, L. J., Gracia-Carpio, J., et al. 2010, MNRAS, 407, 2091
Heckman, T. M. & Best, P. N. 2014, ARA&A, 52, 589
Ivison, R. J., Smail, I., Amblard, A., et al. 2012, MNRAS, 425, 1320
Kennicutt, R. C. & Evans, N. J. 2012, ARA&A, 50, 531
Leroy, A. K., Walter, F., Brinks, E., et al. 2008, AJ, 136, 2782
Leroy, A. K., Walter, F., Sandstrom, K., et al. 2013, AJ, 146, 19
Morganti, R., Robinson, A., Fosbury, R. A. E., et al. 1991, MNRAS, 249, 91
Papadopoulos, P. P., Greve, T. R., Ivison, R. J., & De Breuck, C. 2005, A&A, 444, 813
Salomé, Q., Salomé, P., & Combes, F. 2015, A&A, 574, A34
Schiminovich, D., van Gorkom, J. H., van der Hulst, J. M., & Kasow, S. 1994, ApJ, 423, L101
Solomon, P. M., Downes, D., Radford, S. J. E., & Barrett, J. W. 1997, ApJ, 478, 144
van Breugel, W., Filippenko, A. V., Heckman, T., & Miley, G. 1985, ApJ, 293, 83
van Breugel, W. J. M. & Dey, A. 1993, ApJ, 414, 563